

A Comparison of Wavelength Dependence for Laser-Assisted Lipolysis Effect Using Monte Carlo Simulation

Jong-In Youn, Ph.D

Biomedical Optics Laboratory, Department of Biomedical Engineering,
College of Health and Medical Science, Catholic University of Daegu, Gyeongbuk, South Korea

Abstract

The aim of this study was to evaluate wavelength dependence for laser-assisted lipolysis using a mathematical simulation. In this study, a Monte Carlo simulation was performed to simulate light transport in fat and dermal tissue with 3 different laser wavelengths ($\lambda = 1064$ nm, 1320 nm, and 1444 nm) that are currently used in clinic settings for laser-assisted lipolysis. The relative rates of heat generation versus penetration depth showed that the greatest amount of heat generation was seen in the tissues at $\lambda = 1444$ nm. This Monte Carlo simulation may help lend insight into the thermal events occurring inside the fat and dermal tissue during laser-assisted lipolysis

1. Introduction

As more women and men want to look and feel better about themselves, body contouring and liposculpture continue to grow in popularity, making laser lipolysis one of the most popular cosmetic surgeries performed today [1-4]. Laser lipolysis is usually performed with a cannula that contains a laser fiber. The cannula is inserted into the treatment area and moved back and forth so that the laser energy can dissolve unwanted fat. The immediate effect of laser-assisted lipolysis is to produce temporary pores in the cell membranes of adipocytes, allowing dissolved fat to migrate into the extracellular space [1-4]. Laser lipolysis causes less bleeding, bruising, and swelling than conventional liposuction procedures, resulting in a faster recovery [1-4].

Currently, laser lipolysis is performed in the clinical setting with an Nd:YAG laser at 2 different wavelengths, $\lambda = 1064$ nm (Smartlipo™, Cynosure, Inc., Westford, MA; LipoLite™, Syneron Inc., Irvine CA) and $\lambda = 1320$ nm (CoolLipo™, CoolTouch Corp., Roseville, CA). In this study, a wavelength dependence modeling of the laser lipolysis effect was performed using the 2 popular laser wavelengths in the market, $\lambda = 1064$ nm and 1320 nm, and the recently introduced novel laser wavelength, $\lambda = 1444$ nm (AccuSculpt™, Lutronic Corp., South Korea).

The Monte Carlo simulation technique, which is based on the statistical nature of radiation interactions, has been widely applied in laser radiation transport studies [5-10]. Monte Carlo simulation methods trace the propagation of individual photons through a turbid medium until the photon experiences complete absorption by or escape from the medium [5]. In this study, the heat generation in 2 different homogeneous regions, fat and dermal tissue, was investigated by a computer simulation of

appropriately weighted random absorption and scattering interactions. This mathematical modeling may provide a better understanding of the laser lipolysis process and help to determine the effective wavelength as a function of the fat volume to be removed.

2. Methods

In this study, a Monte Carlo model of laser light distribution in tissue was coded in ANSI standard C. The model is based on calculations describing the heat generation using 3 different wavelengths of laser light ($\lambda = 1064$ nm, 1320 nm, and 1444 nm).

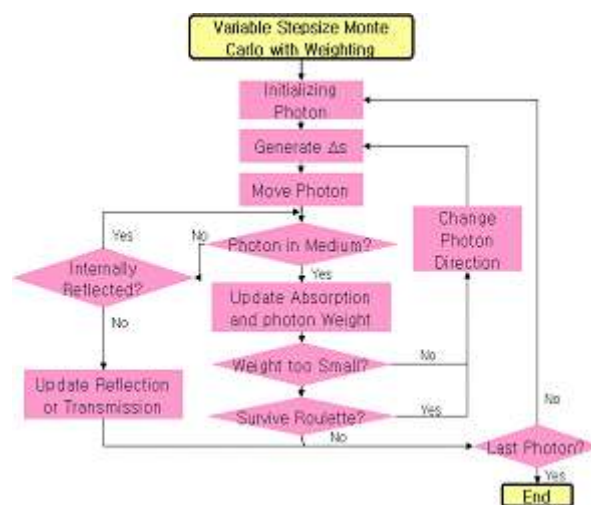


Figure 1. Variable stepsize Monte Carlo with weighting.

Figure 1 shows a flowchart of a Monte Carlo simulation that uses a weighted photon to improve the statistics of the simulation. Each generated photon is moved a distance, Δs , where it may be scattered, absorbed, propagated undisturbed, internally reflected, or transmitted out of the tissue [6-10].

2.1. Initializing the photon

Each photon is initially assigned a weight, W , that is initialized to 1. When a photon is launched, it is first checked at the tissue surface whether or not there is a refractive-index mismatched boundary. Some photons may be specularly reflected, in which case the photon weight is decreased [5].

The specular reflectance is specified as:

$$R_{sp} = \frac{(n_1 - n_2)^2}{(n_1 + n_2)^2} \quad (1)$$

The photon weight is decreased by R_{sp} for the photon to enter the tissue:

$$W = 1 - R_{sp} \quad (2)$$

2.2. Photon Moving

The stepsize of each launched photon, s , is calculated based on a random sampling of the probability distribution for the photon's free path. The computer's random number generator yields a random variable from 0 to 1 [5]. The stepsize is determined by:

$$s = \frac{-\ln \zeta}{\mu_t} \quad (3)$$

Once stepsize is determined, the photon is moved in the tissue. For the photon located at (x, y, z) traveling a stepsize distance in the direction (μ_x, μ_y, μ_z) , the new coordinates (x', y', z') are determined by:

$$\begin{aligned} x' &= x + \mu_x s \\ y' &= y + \mu_y s \\ z' &= z + \mu_z s \end{aligned} \quad (4)$$

2.3. Internal reflectance at the boundary

During each stepsize movement, the photon may hit a boundary. The photon can be either internally reflected by the boundary or escape as observed reflectance. The probability that the photon will be internally reflected is determined by Fresnel's law [5]:

$$R(\theta_i) = \frac{1}{2} \left\{ \frac{\sin^2(\theta_i - \theta_t)}{\sin^2(\theta_i + \theta_t)} + \frac{\tan^2(\theta_i - \theta_t)}{\tan^2(\theta_i + \theta_t)} \right\} \quad (5)$$

Therefore, photon weight that successfully escapes from the tissue is described as:

$$1 - R(\theta_i) \quad (6)$$

2.4. Photon absorption

Once the photon has reached an interaction site, some attenuation of the photon weight owing to absorption by the tissue may occur. The new photon weight is calculated by:

$$W = W \frac{\mu_a}{\mu_t} \quad (7)$$

When photon weight is below the threshold weight, the photon weight becomes 0 and the photon is terminated.

2.5. Photon scattering

When an anisotropy factor (g) value is 0, indicating isotropic scattering, the cosine of the deflection angle is described as:

$$\cos \theta = 2\zeta - 1 \quad (8)$$

When an anisotropy factor (g) value is near 1, indicating anisotropic scattering, the cosine of the deflection angle is described as:

$$\cos \theta = \frac{1}{2g} \left\{ 1 + g^2 - \left(\frac{1 - g^2}{1 - g + 2g\zeta} \right)^2 \right\} \quad (9)$$

This process is repeated according to the total number of photons [3-5].

In this study, 2 different simulation algorithms were used, as described below, at 3 laser wavelengths:

- *Tiny Monte Carlo Simulation*
Simulates light propagation from a point source in an infinite medium with isotropic scattering.
- *Small Monte Carlo Simulation*.
Simulates light propagation from normal irradiation of a semi-infinite medium with anisotropic scattering.

Heat generation is calculated by:

$$Heat [W/cm^3] = \mu_a \frac{3}{4\pi r} \mu_t' P_0 e^{-\sqrt{3\mu_a \mu_t} r} \quad (10)$$

These processes are applied to fat and dermal tissue. Lipolysis efficiency and dermal injury are compared.

Table 1 shows the optical properties of fat and dermal tissue for Monte Carlo simulation variables [8,9].

Table 1. Optical properties of fat and dermal tissue for Monte Carlo simulation variables.

Wavelength	λ (nm)	1064nm	1320nm	1444nm
Fat	μ_a [cm ⁻¹]	1.5	2	2.5
	μ_s [cm ⁻¹]	11	10.5	11
	n	1.37		
	g	0.91		
Dermis	μ_a [cm ⁻¹]	1	2	4
	μ_s [cm ⁻¹]	250	250	250
	n	1.36		
	g	0.91		
Photon #		10000		

Abbreviations: n, refractive index, g, anisotropic factor.

3. Results and Discussion

Tiny Monte Carlo simulation and Small Monte Carlo simulation are performed with fat and dermal tissue.

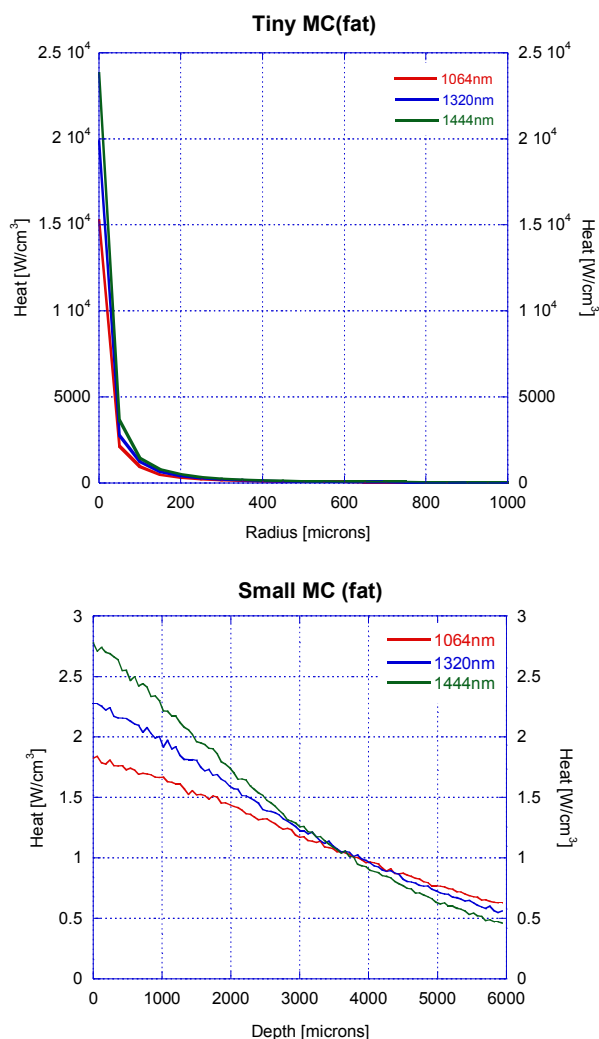


Figure 2. Relative heat generation vs. penetration depth in fat tissue using Monte Carlo (MC) simulations; (upper) Tiny MC, (lower) Small MC.

Figure 2 shows the relative rate of heat generation versus optical penetration depth in fat tissue for the 3 different wavelengths ($\lambda = 1064 \text{ nm}$, 1320 nm , and 1444 nm). In Tiny Monte Carlo simulation with fat tissue, the greatest amount of heat is generated at the surface, but the heat is dramatically reduced as the penetration depth is increased. On the other hand, in Small Monte Carlo simulation, the rate of heat generation in deep fat layers is less than the rate at the surface. These results demonstrated that the highest heat generation in fat tissue was achieved at $\lambda = 1444 \text{ nm}$, followed by, in order, $\lambda = 1320 \text{ nm}$ and 1064 nm . However, the heat generation at $\lambda = 1444 \text{ nm}$ was less than that at $\lambda = 1064 \text{ nm}$ below a depth of 3.5 mm . According to this result, the localized maximum heat generation

for fat tissue can be achieved at $\lambda = 1444 \text{ nm}$, with minimal damage of the surrounding region.

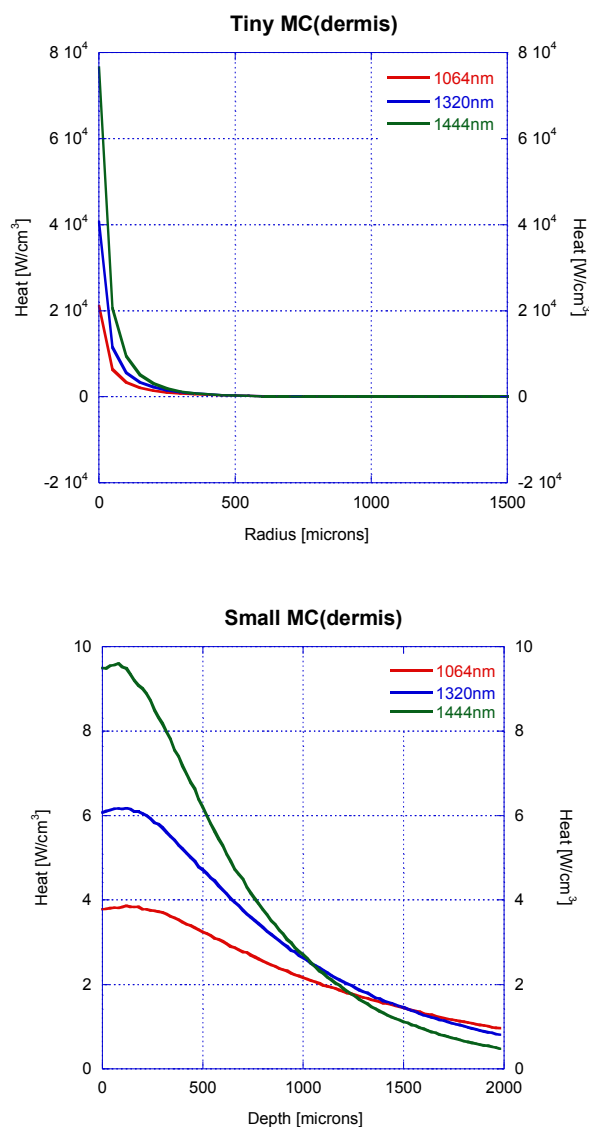


Figure 3. Relative heat generation vs. penetration depth in the dermis using Monte Carlo (MC) simulations; (upper) Tiny MC, (lower) Small MC.

Figure 3 presents the results from Tiny Monte Carlo and Small Monte Carlo simulations of the dermis. As with Monte Carlo simulations of fat tissue (Figure 2), the highest heat generation was achieved at $\lambda = 1444 \text{ nm}$, followed by, in order, $\lambda = 1320 \text{ nm}$ and 1064 nm . In the same manner, localized maximum heat generation for dermal tissue can be achieved at $\lambda = 1444 \text{ nm}$, with minimal damage of the surrounding region because the heat generation at $\lambda = 1444 \text{ nm}$ is less than that at $\lambda = 1064 \text{ nm}$ below a depth of 1.2 mm .

Laser lipolysis is performed by inserting a cannula into the fat layer under the skin. There is little likelihood that the procedure results in thermal or mechanical damage to the dermis. The results from Monte Carlo simulation for both fat

and dermal tissue suggest that injury will be greater with the 1444-nm laser than with the other 2 wavelengths, $\lambda = 1064$ nm and 1320 nm. However, the minimal localization of heat at $\lambda = 1444$ nm for both fat and dermal tissue using laser-assisted lipolysis means that the thermal damage in the surrounding tissue is likely to be minimal.

4. Conclusion

In this study, the wavelength dependence of laser-assisted lipolysis was simulated using the Monte Carlo statistical method with 3 different wavelengths, $\lambda = 1064$ nm, 1320 nm, and 1444 nm. The simulation was performed with homogeneous fat and dermal tissue, and the heat generation for both types of tissue over the penetration depth was investigated. The results show that the greatest amount of heat generation is observed in both types of tissue at $\lambda = 1444$ nm, followed by, in order, $\lambda = 1320$ nm and 1064 nm. Consequently, $\lambda = 1444$ nm shows the highest ablation efficiency, with minimal localization of heat over the depth, when compared with the other 2 wavelengths, $\lambda = 1320$ nm and 1064 nm, for laser-assisted lipolysis.

5. Reference

1. Apfelberg DB, Rosenthal S, Hunstad JP, Achauer B, Fodor PB. Progress report on multicenter study of laser-assisted liposuction. *Aesthetic Plast Surg* 1994; 18(3): 259-264.
2. Apfelberg DB. Results of multicenter study of laser-assisted liposuction. *Clin Plast Surg* 1996; 23(4): 713-719.
3. R. R. Anderson, W. Farinelli, H. Laubach, D. Manstein, A. N. Yaroslavsky, J. Gubeli, K. Jordan, G. R. Neil, . Shinn, W. Chandler, G. P. Williams, S. V. Benson, D. R. Douglas, H. F. Dylla, Selective Photothermolysis of Lipid-Rich tissues: A Free Electron Laser study, *Lasers Surg and Med* 2006; 38:913-919.
4. J. G. Khoury, R. Saluja, D. Keel, S. Detwiler, M. P. Goldman, Histologic Evaluation of Interstitial lipolysis comparing a 1064, 1320 and 2100nm laser in an Ex Vivo Model, *Lasers Surg and Med* 2008; 40:402-406.
5. A.J. Welch, M.J.C. van Gemert *Optical-Thermal Response of Laser-irradiated Tissue*, Plenum Press, New York, 1995.
6. L. Wang, S. L. Jacques, L. Zheng, Monte Carlo Modeling of light transport in multi-layered tissues, *Computer methods and programs in biomedicine* 1995; 47:131-146.
7. S. A. Prahl, M. Keijzer, S. L. Jacques, A. J. Welch, A Monte Carlo Model of Light Propagation in Tissue, *SPIE Institute Series* 1989; Vol. IS 5.
8. Bashkatov AN, Genina EA, Kochubey VI, Tuchin VV. Optical Properties of the Subcutaneous Adipose Tissue in the Spectral Range 400-2500nm. *Geometrical and Applied Optics*. 2005; 99(5):868-874.
9. S. R. Mordon, B. Wassmer, J. P. Reynaud, J. Zemmouri, Mathematical modeling of laser lipolysis, *BioMedical Engineering OnLine*. 2008; 7:10.
10. A. J. Welch, C. M. Gardner, Monte Carlo Model for determination of the Role of Heat generation in Laser-irradiated Tissue, *Journal of Biomedical Engineering*, 1997; Vol. 119.